

a little further in order to point out an apparent anomaly in the use of hybrid modes.

In addition to the problem just discussed, six-component hybrid modes have been found to be necessary for general solutions in ferrite-loaded rectangular waveguides<sup>8,9</sup> and in rod-loaded, dielectric or ferrite, circular guides.<sup>8,10</sup> Hybrid mode solutions have been found by taking linear combinations of TE and TM modes in each region and matching all fields parallel and fluxes normal to the discontinuity; in practice, it is necessary to match only four components to achieve this. To check this method, we will compare the results obtained in a particular problem which is solved by both hybrid and LS modes.

Consider an isotropic, rectangular waveguide divided into two transverse regions having different dielectric and magnetic properties. The interface, in the  $x$ - $z$  plane, occurs at  $y=c$  and the guide sidewalls are at  $y=0$  and  $y=b$ . Propagation is in the  $z$  direction. The TE and TM solutions are known in each region and are to be combined in proportions to be determined by matching considerations. There are four unknown amplitude constants. By matching four field components across the boundary, the unknown constants may be eliminated, resulting in an eigenvalue equation.

Matching  $E_z$ ,  $H_z$ ,  $E_x$ , and  $H_x$  at  $y=c$  we find after some algebraic manipulation, that

$$\frac{\epsilon_1 k_{y1} (k_x^2 + k_{y2}^2) \cdot \cot k_{y1} c + \epsilon_2 k_{y2} (k_x^2 + k_{y1}^2) \cdot \cot k_{y2} (b - c)}{\mu_1 k_{y1} (k_x^2 + k_{y2}^2) \cdot \tan k_{y1} c + \mu_2 k_{y2} (k_x^2 + k_{y1}^2) \cdot \tan k_{y2} (b - c)} = \frac{k_x^2 k_z^2 (k_z^2 - k_1^2) (\mu_1 \epsilon_1 - \mu_2 \epsilon_2)}{\mu_1 k_{y1} (k_x^2 + k_{y2}^2) \cdot \tan k_{y1} c + \mu_2 k_{y2} (k_x^2 + k_{y1}^2) \cdot \tan k_{y2} (b - c)} \quad (49)$$

where the cutoff relation is

$$k_x^2 + k_y^2 + k_z^2 = k^2 \quad (50)$$

and

$$k_z = -j\Gamma. \quad (51)$$

The subscripts 1 and 2, on  $k_y$  and  $k$ , refer to the regions in which  $0 < y < c$  and  $c < y < b$ , respectively.  $k_x$  and  $k_z$  must be the same in both regions so that the fields will be matched for all  $x$  and  $z$ .  $k_x$  is given by (44).

If now,  $E_z$ ,  $H_z$ ,  $E_x$ , and  $D_y$  are matched, (52) results.

$$\frac{\mu_1 k_{y1} (k_x^2 + k_{y2}^2) \cdot \cot k_{y2} (b - c) + \mu_2 k_{y2} (k_x^2 + k_{y1}^2) \cdot \cot k_{y1} c}{\epsilon_1 k_{y1} (k_x^2 + k_{y2}^2) \cdot \tan k_{y2} (b - c) + \epsilon_2 k_{y2} (k_x^2 + k_{y1}^2) \cdot \tan k_{y1} c} = \frac{k_x^2 (k_z^2 - k_1^2) [\mu_2 \epsilon_2 (k_x^2 + k_{y1}^2) - \mu_1 \epsilon_1 (k_x^2 + k_{y2}^2)]}{\epsilon_1 k_{y1} (k_x^2 + k_{y2}^2) \cdot \tan k_{y2} (b - c) + \epsilon_2 k_{y2} (k_x^2 + k_{y1}^2) \cdot \tan k_{y1} c}. \quad (52)$$

The eigenvalue equations (49) and (52) are both rather involved. We know, on firm theoretical grounds, that LS modes should give correct results. Therefore, using LSM and LSE modes respectively, the following are found:

$$\frac{\epsilon_2}{\epsilon_1} = -\frac{k_{y2} \cot k_{y1} c}{k_{y1} \cot k_{y2} (b - c)} \quad (53)$$

$$\frac{\mu_2}{\mu_1} = -\frac{k_{y2} \cot k_{y2} (b - c)}{k_{y1} \cot k_{y1} c}. \quad (54)$$

<sup>8</sup> G. Brazilai and G. Gerosa, "Modes in rectangular guides filled with magnetized ferrite," *Nuovo Cimento*, vol. 7, p. 685, 1958.

<sup>9</sup> B. Lax and K. J. Button, *Microwave Ferrites and Ferrimagnetics*. New York: McGraw-Hill, 1962, pp. 388-399.

<sup>10</sup> P. J. B. Clarricoats, "Propagation along unbounded and bounded dielectric rods," (two parts.), *Proc. IEE (London)*, vol. 108C, pp. 170-86, March 1961.

These hold for all  $k_z$ . To be sure that (52) is not the same as (54), a numerical solution of the latter was substituted into the former and found not to be satisfactory. This must almost certainly be true of (49) and (53) as well. Even though the fields are completely matched in all cases, the eigenvalue equations obtained are inconsistent!

As a variant of the previous hybrid approach, six-component hybrid modes were formed by taking combinations of LSE and LSM modes (where before, TE and TM pairs were used). First of all,  $D_y$  and  $B_y$  were matched. Then, when  $E_z$  and  $F_z$  were matched, (53) resulted; when  $H_z$  and  $H_x$  were matched, (54) was obtained. No disagreement appears here as the eigenvalue equations turn out correctly.

It is difficult to believe that (49) and (52) are completely wrong. After all, they were derived from modes that individually satisfied Maxwell's equations in the homogeneous regions and, taken in pairs, the internal boundary as well. Note that (53) and (54) result from (49) and (52) when  $k_z=0$  is substituted. Although this condition is not physically realizable for LSM modes and is unduly restricting for LSE modes, it suggests that there are particular values of  $k_z$  (not necessarily zero) for which correct solutions of (49) and (52) may be found. It is likely that these roots correspond to a restricted range of solutions and there-

Altschuler<sup>1</sup> provides a simple method of determining the cutoff frequency, which is readily obtainable from the phase constant of the waveguide. However, if a more accurate determination is required, the preceding method may not be adequate. A more accurate and convenient method for determining cutoff frequencies is presented here.

It is assumed that the waveguide under consideration is uniform, cylindrical, and with an arbitrary cross section. It is possible to form a resonant cavity by shorting both ends of a guide. Through an iris in one of the shorts, energy is fed into the cavity, and resonance is observed using a directional coupler and a detector setup as shown in Fig. 1. Let  $f_0$  and  $f_q$  be two resonant frequencies of the cavity with  $f_q$  larger than  $f_0$ . The two resonant modes must be in the same transverse variation with only the number of longitudinal variations differing by an integer  $q$ . In other words, if  $m$  and  $n$  represent the transverse variational numbers, and  $p$  represents that of the longitudinal, then  $f_0$  is in the  $(m, n, p)$  mode, and  $f_q$  is in the  $(m, n, p+q)$  mode.

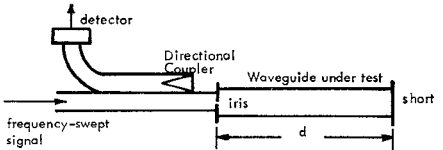


Fig. 1. Simplified diagram for observing cavity resonance.

The electrical length of a waveguide with two ideal shorts on both ends is a multiple of  $\pi$  radians. However, due to the coupling iris in one of the shorts, the length differs from the ideal case by a fraction  $\delta_0$ . At the resonant frequency  $f_0$ , the electrical length is expressed as follows:

$$\beta_0 d = (N - \delta_0) \pi \quad (1)$$

where  $\beta_0$  is the phase constant,  $d$  is the physical length of the line, and  $N$  is an integer.

The physical length of the cavity at resonance is a multiple of half guide wavelengths. In a similar argument<sup>2</sup> the length is

$$d = (N - \delta_0) \lambda_0 / 2 \quad \text{at } f_0 \quad (2)$$

and

$$d = (N - \delta_q + q) \lambda_q / 2 \quad \text{at } f_q \quad (3)$$

where  $\lambda_0$  and  $\lambda_q$  are the guide wavelengths at  $f_0$  and  $f_q$ , respectively. Using (1)-(3) and eliminating  $N$  results into

$$2d = (q + \delta_0 - \delta_q) \lambda_q \lambda_0 / (\lambda_0 - \lambda_q). \quad (4)$$

If the frequency range of operation is not too wide, the fractions  $\delta_0$  and  $\delta_q$  are almost equal, as will be demonstrated later. Equation (4), therefore, reduces to

$$q/2d = 1/\lambda_q - 1/\lambda_0 \quad (5)$$

<sup>1</sup> H. M. Altschuler, "Attenuation and phase constants," in *Microwave Measurements*, vol. 3, M. Sucher and J. Fox, Eds. New York: Polytechnic Press of Polytechnic Inst. of Brooklyn, 1963, ch. 6.

<sup>2</sup> H. M. Barlow and A. L. Cullen, *Microwave Measurements*. London, England: Constable and Co. Ltd., 1950, ch. 3.

## Measurement of Cutoff Frequencies

Measurements of guide wavelengths and cutoff frequencies are often of interest in experimental investigations of waveguides with general cross sections. When necessary measuring equipment is not available, the phase constant measurement described by

Manuscript received July 1, 1965. The work reported here was supported by the National Aeronautics and Space Administration partially funded under NsG-381.

and it is independent of  $\delta$ , i.e., independent of the coupling iris. Expressing the guide wavelength of (5) in terms of resonant and cutoff frequencies, and after simple algebraic manipulations, the cutoff frequency of the waveguide is expressed as follows:

$$f_c^2 = f_q^2 - [A/4 + (f_q^2 - f_0^2)/A]^2 \quad (6)$$

where  $A = qc/d$ , and  $c = 2.99792 \times 10^8$  meters/s.

It should be noted that the accuracy of (6) depends on the measurement of the resonant frequencies  $f_q$  and  $f_0$ . For long sections of waveguide, two adjacent resonant frequencies ( $q=1$ ) are so close together that commercial wave meters cannot give accurate resolution. It is suggested, therefore, that investigations be performed on relatively short sections and that  $q$  be taken greater than one.

A 2.996-inch *K*-band (WR-42) waveguide section was shorted on both ends with a  $\frac{1}{4}$ -inch coupling hole made at the center of one end plate. The cavity has six resonant frequencies in this band, with the first and the sixth resonances occurring at 18.341 Gc/s and 25.798 Gc/s, respectively. The cutoff frequency calculated by (6) is 14.053 Gc/s (with  $q=5$ ), with accuracy up to five significant figures, compared with the exact value 14.051 Gc/s. The value of the difference  $\delta_q - \delta_0$  is in the order of  $10^{-6}$ , and the magnitude of  $\delta$  is about 0.032. The average of six cutoff frequencies each calculated for a measured resonant frequency by the phase constant method is 14.014 Gc/s. One reason for the discrepancy is due to not taking  $\delta$  into account.

To demonstrate the fact that the cutoff frequency measurement is independent of the coupling hole, a vertical slit was cut in the short. The first and sixth resonant frequencies were 18.348 Gc/s and 25.810 Gc/s, respectively, and the cutoff frequency was 14.047 Gc/s which is only 6 Mc/s less than the first calculation.

N. F. AUDEH

H. Y. YEE

Research Inst.  
University of Alabama  
Huntsville, Ala.

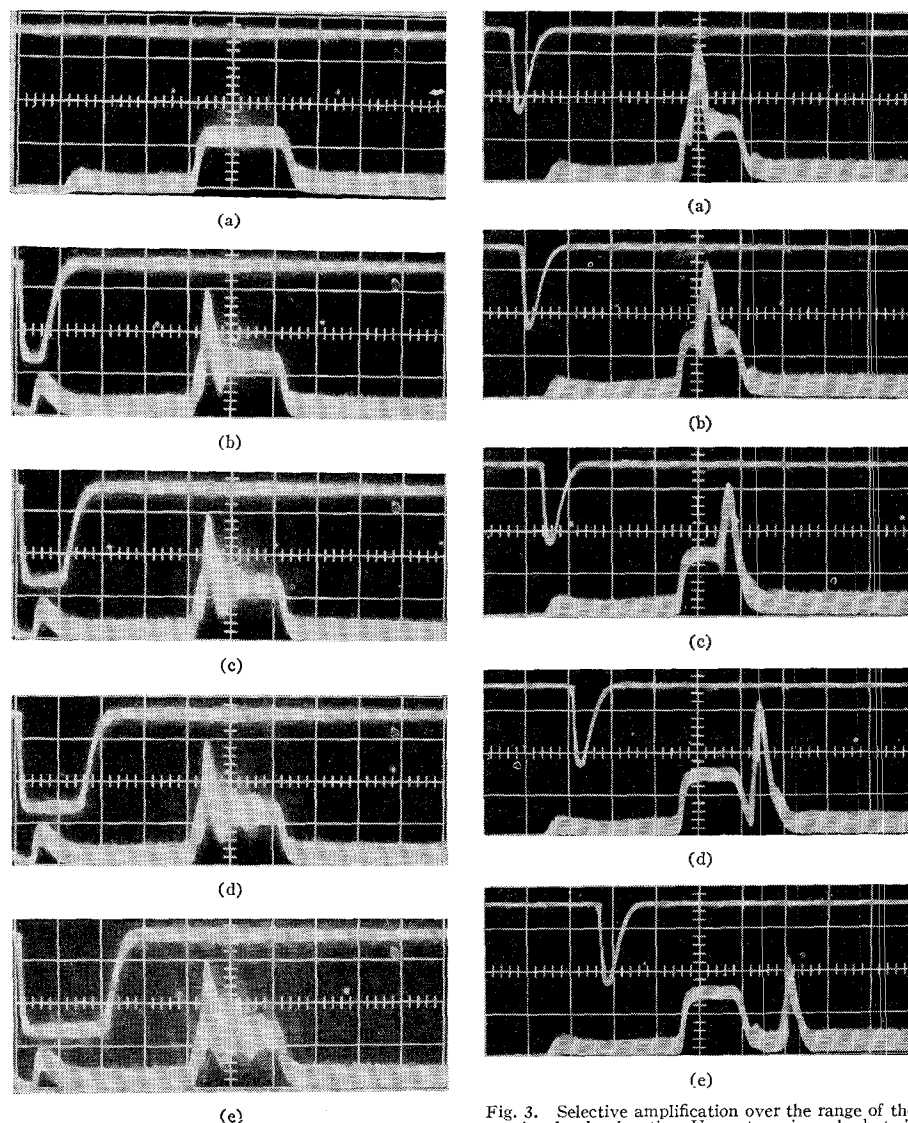


Fig. 1. Oscilloscope photographs showing independence of transient gain on pump pulse width. Upper trace in each photo is video detected pump pulse. Lower traces: signal frequency 1 Gc/s; pump frequency 2 Gc/s; input signal level 13 dBm; pump power 1.5-watt peak; signal pulse width 2  $\mu$ s; pump, pulse width (a) pump off, (b) 0.5  $\mu$ s, (c) 1.0  $\mu$ s, (d) 1.5  $\mu$ s, (e) 2.0  $\mu$ s, horizontal time 1  $\mu$ s/cm, dc magnetic field 1200 Gauss.

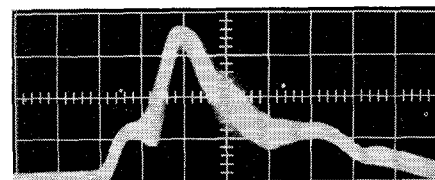


Fig. 2. Expanded view of transient gain phenomenon. Signal frequency 1 Gc/s; pump frequency 2 Gc/s; input signal level 13 dBm; pump power 1.5-watt peak; signal pulse width 2  $\mu$ s; pump pulse width 1  $\mu$ s; dc magnetic field 1200 Gauss; horizontal time base 0.4  $\mu$ s/cm.

## Characteristics of Transient Parametric Amplification of Elastic Waves in YIG

The observation of a transient mode of quasi-degenerate parametric amplification of elastic waves in YIG was reported<sup>1</sup> in an earlier letter along with other modes of operation. The purpose of this correspondence is to describe further experiments that

Manuscript received July 9, 1965. The research reported here was supported in part by the Rome Air Development Center, Griffiss Air Force Base, N. Y., under Contract AF 30(602)-3611.

<sup>1</sup> R. A. Sparks, and E. L. Higgins, "CW pumped and nondegenerate parametric amplification of elastic waves in YIG," *Appl. Phys. Letters*, vol. 7, pp. 41-43, July 15, 1965.

have been conducted in order to characterize in greater detail the very high gain, transient amplification process in the microwave frequency range.

As in the previously reported measurements, thin wire excitation was used at both ends of the [111] oriented YIG crystal bar

Fig. 3. Selective amplification over the range of the signal pulse duration. Upper trace in each photo is video detected pump pulse. Lower traces: signal frequency 1 Gc/s; pump frequency 2 Gc/s; input signal level 13 dBm; pump power 1.5-watt peak; signal pulse width 1.5  $\mu$ s; pump pulse width 0.5  $\mu$ s; horizontal time 1  $\mu$ s/cm; dc magnetic field 1200 Gauss.

that measured 1.48 cm in length and 0.33 cm on each side. All of the data was taken by observing the reflected pulses at the signal input end of the bar. The signal frequency was maintained at 1 Gc/s and the pump frequency held constant at approximately 2 Gc/s. For an RF signal input level of -13 dBm and a magnetic bias field aligned parallel to the bar axis of 1200 Gauss, three elastic wave pulses were detectable with no pump power applied. The pulses were separated in time by an interval corresponding to the velocity of propagation<sup>2</sup> of transverse elastic waves in YIG.

With the signal pulse width maintained constant at 2  $\mu$ s, the series of oscilloscope photographs shown in Fig. 1 was taken. In Fig. 1(a) the pump frequency was turned off, and in Fig. 1(b) through (e) the pump frequency was turned on with pulse widths

<sup>2</sup> A. E. Clark and R. E. Strakna, "Elastic constants of Single-Crystal YIG," *J. Appl. Phys.*, vol. 32, pp. 1172-1173, June 1961.